FERMILAB-PROPOSAL-0888

cy ltr mc
cf

888

INDIANA UNIVERSITY

(812) 855-6537/2878
(812) 855-6645 (fax)
e-mail: vicv@iucf.indiana.edu

July 10, 1996

DIRECTOR'S OFFICE
JUL 1 5 1996

COLLEGE OF
ARTS AND SCIENCES

Dr. John Peoples, Director
Fermilab
P.O. Box 500
Batavia, IL 60510

Dear Dr. Peoples:

Enclosed you will find a letter of intent for studies of the nuclear equation-of-state with antiproton beams at Fermilab. Since we are new to the Fermilab environment, we would appreciate learning the steps necessary to convert this document into a full proposal--if it is found technically feasible by your staff.

Also, we would like to express our thanks to Chuck Brown, Mike Church, Jeff Appel and Linda Stuttle for helping us get plugged into Fermilab. Their interest and advice on technical matters was greatly appreciated.

Sincerely,

Vic Viola

V. E. Viola
Distinguished Professor
of Chemistry

VV:kb

DEPARTMENT OF CHEMISTRY

Chemistry Building
Bloomington, Indiana
47405-4001

Fax: 812-855-8300

888

LETTER OF INTENT

$\bar{p}$ + A STUDIES OF THE NUCLEAR EQUATION-OF-STATE

Submitted by: K. Kwiatkowski and V. E. Viola, Indiana University

Collaborating Institutions:

CEA Saclay
University of Maryland
Simon Fraser University
Texas A & M University

$\bar{p}$ + A STUDIES OF THE NUCLEAR EQUATION OF STATE

I. Physics Justification

Determining the properties of hadronic matter as a function of temperature, density and neutron-proton composition is one of the fundamental goals of nuclear physics. The resulting nuclear equation of state (EOS) is essential not only for understanding the physics of complex nuclei, but also for describing astrophysical systems--for example, the aggregation of low-density hadronic matter to form stars, and the subsequent evolution of such bodies into supernovae, neutron stars and black holes.

Central collisions between hadron projectiles and heavy nuclei are unique in that they create highly excited nuclei with minimal compression. The heating mechanism proceeds via hard N-N scattering and the multiple excitation of baryonic resonances in the core of the nucleus--temporarily creating a region of locally concentrated resonance matter, a possible precursor of the quark-gluon plasma. The rapid evolution of such systems into regions of phase instability is indicated in Fig. 1. Here the collision trajectory predicted by a BUU calculation [Wa-96, Da-95] is traced in the temperature/density/entropy per nucleon phase diagram for infinite nuclear matter [Mu-95]. Time steps are in units of 4 fm/c and the trajectory density is the maximum (not average), reflecting the projectile momentum front. The calculations indicate that the nucleus is rapidly heated to energies well in excess of the total nuclear binding energy, followed by mass loss and expansion into the liquid-gas coexistence and spinodal instability regions on a time scale that is much shorter than that for collective nuclear response. The BUU simulations also suggest that at the end of the fast cascade/resonance deexcitation stage, a region of depleted density, or cavity, exists in the core of the nucleus, as illustrated in Fig. 2.

The exploration of the nuclear EOS with antiproton beams affords a major advantage in that one benefits from the simplicity of hadron projectiles, while significantly enhancing the excitation energy deposited in the residual nucleus. This enhancement derives from the pions associated with the antiproton annihilation ($m_\pi \sim 5$), which further enrich the "resonance matter" composition in the nuclear interior. Fig. 3 shows transport model predictions for the average nuclear excitation imparted to a gold nucleus by an antiproton beam. Relative to that for protons and negative pions, the antiproton deposition energy is 30 - 40% greater [To-95]. The calculations predict that the optimum beam momentum for reabsorbing the pions and resonances created in the initial N-N collision volume occurs at about 6 - 8 GeV/c. At higher momenta, lack of nuclear stopping leads to significant pion escape and a saturation of the deposition energy. This additional excitation afforded by $\bar{p}$ projectiles is highly significant in that, if correct, it would permit investigation of the nuclear vaporization regime of the caloric curve, as postulated by workers at GSI and shown in Fig. 4. At present, it appears that data from proton, pion, and ^{3}He projectiles, just reach this critical vaporization limit at energies per nucleon greater than 10 MeV, but do not sample the region beyond that to any significant extent.

In summary, studies of the nuclear EOS require the highest possible nuclear excitation with good source definition. As pointed out by Cugnon [Cu-94], the antiproton is the best probe for fulfulling these requirements. Further, our Indiana Silicon Sphere 4π detector array (ISiS) is

the only existing detector capable of performing multifragmentation measurements with antiproton beams.

II. Summary of Previous p + A Studies

During the past 2½ years, our group has completed three major investigations of hadron and light-ion-induced reactions with the ISiS array. A description of the array is appended. These experiments include:

(1) E375 at IUCF--Studies of non-equilibrium nuclear dynamics between the Fermi energy and pion threshold in proton and ^{3}He-induced reactions between 100 and 270 MeV; and

(2) E228 at LNS Saclay--Studies of multifragmentation in the Δ-resonance regime with 1.8 - 4.8 GeV ^{3}He + Ag, Au reactions. Letters describing early results are appended.

(3) E900 at AGS--Multifragmentation in the limiting fragmentation regime with hadron beams from 5 to 15 GeV/c.

During the 1996 proton cycle at AGS, the ISiS array was successfully installed on the C5 beam line, along with a halo rejection system fabricated at Simon Fraser University and Indiana University and beam diagnostics provided largely by AGS. Tests of the system during the first week of March demonstrated that ISiS could function with good particle identification and energy resolution for H and He isotopes and intermediate-mass fragments (IMF: $2 < Z < 15$) at acceptable count rates. Fig. 5 shows representative charged-particle multiplicity distributions and particle identification spectra obtained on-line during the run.

Data acquisition began at the end of the first week of March and we subsequently completed multifragmentation studies of the following systems:

•Positive beam: "p" + ^{197}Au at 6.0 (70% π^+), 10.0, 12.8 and 14.6 GeV/c, and

•Negative beam: "π^-" + ^{197}Au at 5.0, 8.0 and 9.2 GeV/c.

More than 1 million events with charged particle multiplicity $M > 6$ were obtained for all systems except the 6.0 GeV/c protons, where only about 3×10^5 events were collected.

While off-line data analysis is just beginning, several preliminary physics results can be deduced from on-line analysis of the data. These include:

(1) The charged-particle and IMF multiplicity distributions for proton and π^- beams are nearly identical at the same beam momentum (Fig. 6), suggesting that energy deposition is similar for both projectiles. The concordance between the data of Fig. 6 and the calculations shown in Fig. 3 provide confidence that antiproton beams will yield the significantly enhanced nuclear excitation required for these EOS studies.

(2) These results, both in relation to data and theory comparisons, are in general accord with our 4.8 GeV ^{3}He + ^{197}Au data obtained previously at LNS Saclay [Kw-95, Mo-95].

(3) The average charged-particle and IMF multiplicities are not strongly dependent on beam momentum between 5 and 14.6 GeV/c. This also is consistent with the transport calculations of Fig. 3.

III. Proposed FNAL Program

The long-term goal of this letter of intent is to study the excitation function for $\bar{p}$-induced reactions on ^{197}Au nuclei. We plan to propose measurements at momenta of 2, 5, 8, 12, and 20 GeV/c; approximately 1 x 10^{12} total $\bar{p}$'s incident on a 1 x 1 cm^2 target would be required at each energy. Our highest priority is the 8 GeV/c beam, which would correspond to the onset of deposition-energy saturation in Fig. 3. However, the calculations indicate that higher $\bar{p}$ energies would also produce similar heating of the nucleus. The 2 GeV/c measurements would examine the results of similar studies at LEAR that were performed with a detector having a reduced acceptance compared to ISiS. The ISiS array can function either on the $\bar{p}$ accumulator ring or on a secondary beam line.

In terms of floor space, the layout for E900 at AGS shown in Fig. 7 illustrates our needs. A flight path of ≥ 30 m, preferably in vacuum, would be necessary for adequate beam tagging if placed on a secondary beam line. Space for a forward array ~ 10 m downstream from the ISiS array (± 3 m each side) is desirable, but not essential. More critical is that we are not downstream from a beam dump on another line. Since our electronics are mounted adjacent to the detector array, it is important to have some means of temperature and humidity control around the localized area of the array; e.g. a plastic tent with some heating/AC capability, depending on the time of year. For data acquisition, we would require an Ethernet line and counting house space of ~ 100 - 150 ft^2. Setup time for the entire system is about one month.

Our only possible safety concerns are (1) the C_3F_8 gas used in our ion-chambers; C_3F_8 is inert and a non-ozone-depleting gas, and (2) ^{241}Am alpha-particle spectroscopy sources for silicon calibration; these are < 10^4 dps.

References

[Cu-94] J. Cugnon, Phys. of At. Nucl. 57, 1635 (1994).

[Da-95] P. Danielewicz, Phys. Rev. C 51, 716 (1995); P. Danielewicz and G. Bertsch, Nucl. Phys. A 533, 712 (1991).

[Kw-95] K. Kwiatkowski et al., Phys. Rev. Lett. 74, 3756 (1995).

[Mo-95] K. B. Morley et al., Phys. Lett. B 355, 52 (1995).

[Mu-95] H. Müller and B. D. Serot, Phys. Rev. C 52, 2072 (1995).

[To-95] V. Toneev, private communication of quark-gluon string model code, 1995.

[Wa-96] G. Wang et al., Phys. Rev. C 53, 1811 (1996).

Figure Captions

Figure 1. Properties of infinite nuclear matter with $y = Z/A = 0.4$ as a function of density, temperature and entropy per baryon [Mu-95]. The solid curves denote the coexistence curve (CE), the diffusive spinodal (DS), the isothermal spinodal (ITS) and the adiabatic spinodal (AS). The point CP identifies the critical point. Also indicated are schematic trajectories for p + A reaction in steps of 4 fm/c, based on a BUU simulation for central collisions (b = 0) [Da-95].

Figure 2. BUU [Da-95] calculation of nuclear matter density contours for the 5 GeV + ^{197}Au reaction as a function of time. Contours are for a cut through the center of the nucleus (x, z plane) along the beam direction (z). From [Wa-96].

Figure 3. Average excitation energy for π^-, p and $\bar{p}$ beams incident on ^{197}Au as a function of projectile momentum. Calculation is the quark-gluon string model of Toneev [To-95], averaged over impact parameter.

Figure 4. The "caloric curve" obtained from peripheral ^{197}Au + ^{197}Au reactions (from Po-95), which plots the dependence of isotope-ratio temperatures T_{HeLi} versus excitation energy per nucleon. The solid line represents Fermi gas with a = 10 MeV^{-1} and the dashed line is for a classical gas of elementary particles, offset by 2 MeV.

Figure 5. Particle-identification spectrum in ISiS telescopes for four hours of data: (a) single ion chamber/silicon telescope; (b) superimposed sum of 158 ion chambers/silicon telescopes, normalized on-line to alpha punch-through energy; (c) single silicon/CsI telescope, and (d) charged-particle multiplicity distribution spectra for several systems, as indicated on figure, measured in '96 E900 run.

Figure 6. Average IMF multiplicity as a function of total beam energy for p + Au and π^- + Au reactions (preliminary 6.0 GeV/c p data are consistent with these data).

Figure 7. Layout of ISiS array for E900 at AGS.

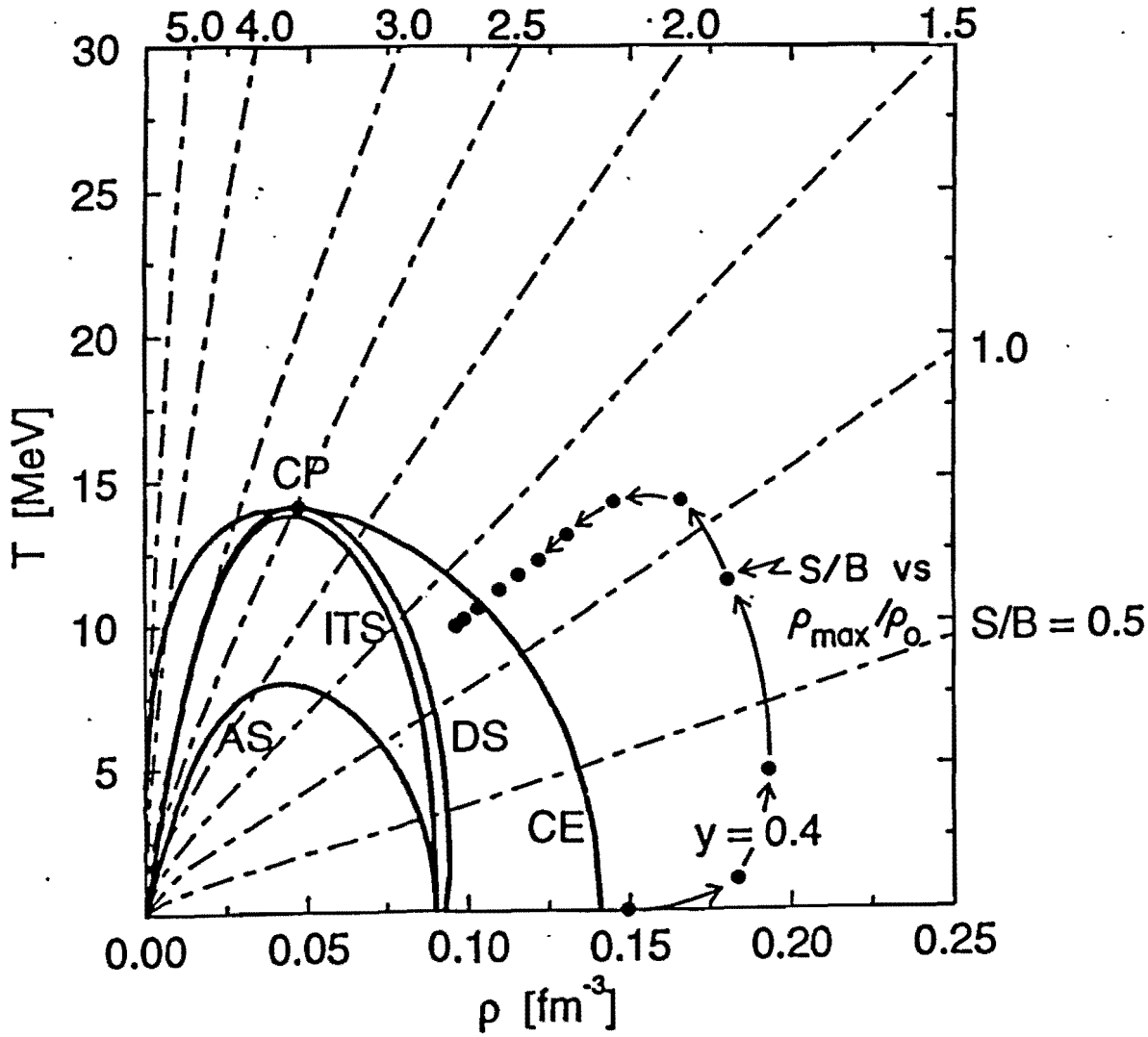
5.0
4.0
3.0
2.5
2.0
1.5
1.0
S/B = 0.5
30
25
20
15
10
5
T [MeV]
CP
ITS
AS
DS
CE
S/B vs
ρ_{max}/ρ_0
y = 0.4
0.00
0.05
0.10
0.15
0.20
0.25
ρ [fm^{-3}]

Fig. 1

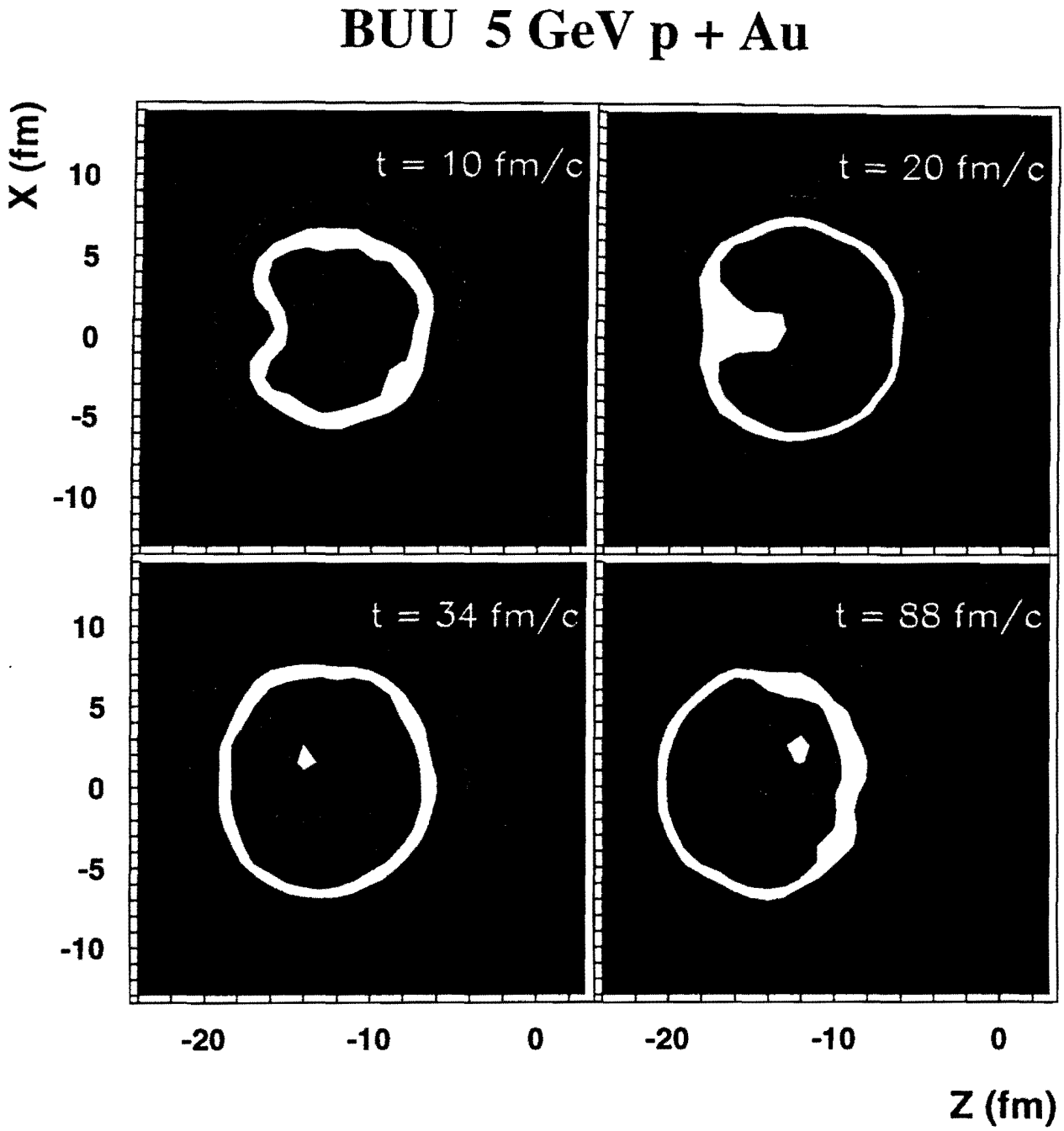
BUU 5 GeV p + Au
X (fm)
10
5
0
-5
-10
t = 10 fm/c
t = 20 fm/c
t = 34 fm/c
t = 88 fm/c
-20
-10
0
Z (fm)

Fig. 2

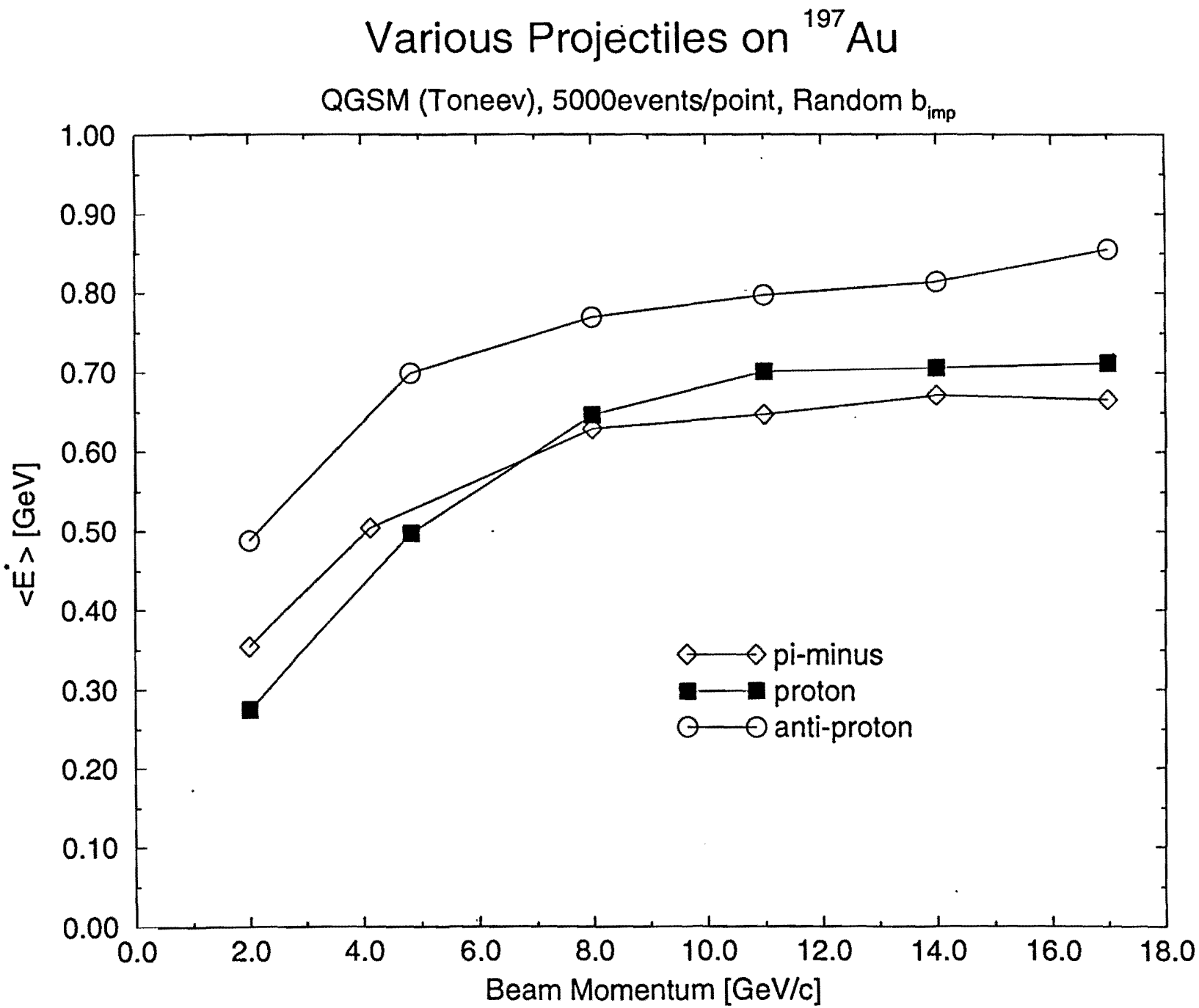
Various Projectiles on 197Au
QGSM (Toneev), 5000events/point, Random b_imp
<E*> [GeV]
Beam Momentum [GeV/c]
pi-minus
proton
anti-proton
1.00
0.90
0.80
0.70
0.60
0.50
0.40
0.30
0.20
0.10
0.00
0.0
2.0
4.0
6.0
8.0
10.0
12.0
14.0
16.0
18.0

Fig. 3

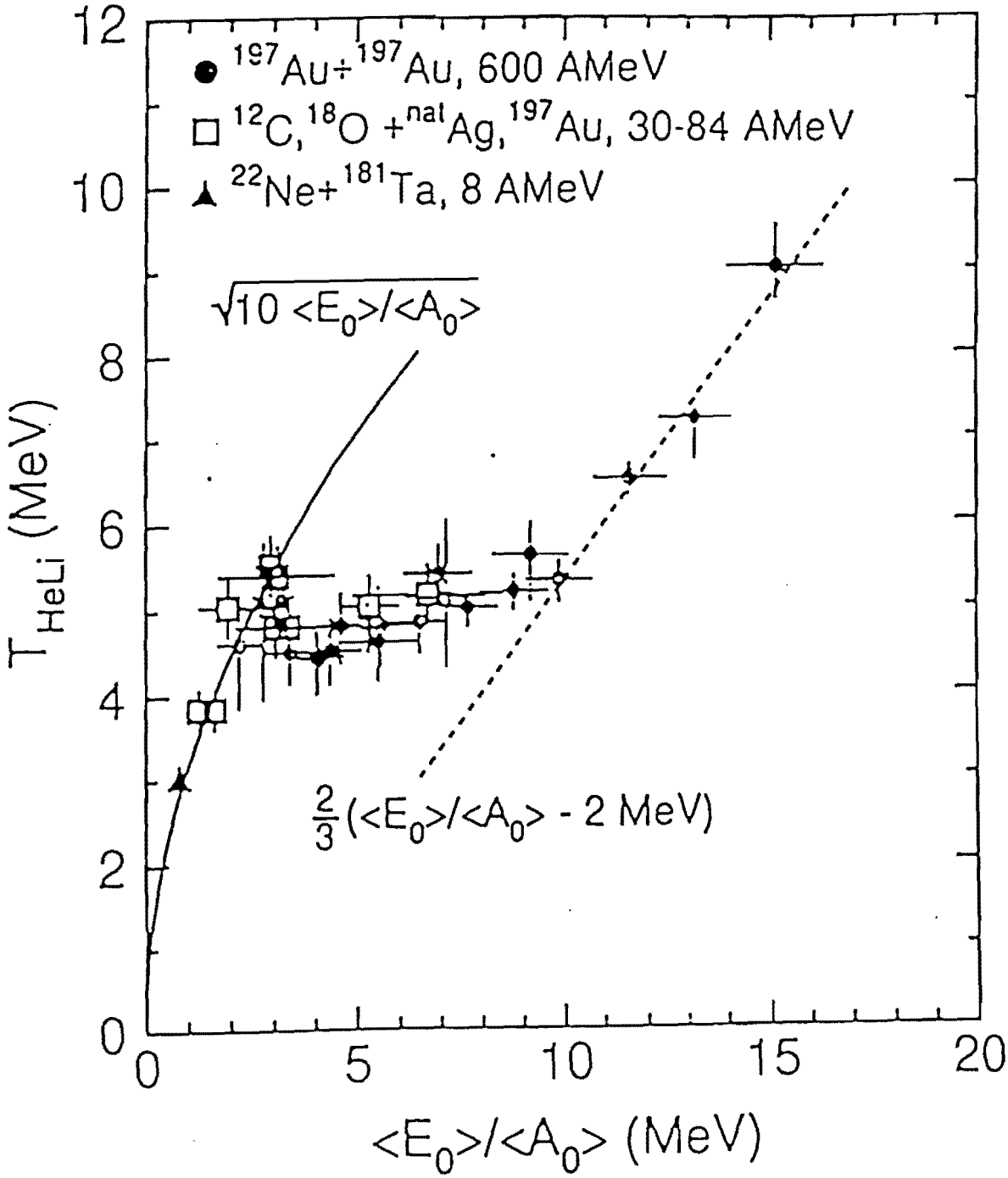
^{197}Au+^{197}Au, 600 AMeV
^{12}C,^{18}O +^{nat}Ag,^{197}Au, 30-84 AMeV
^{22}Ne+^{181}Ta, 8 AMeV
$\sqrt{10 <E_0>/<A_0>}$
$\frac{2}{3}(<E_0>/<A_0> - 2$ MeV)
T_{HeLi} (MeV)
$<E_0>/<A_0>$ (MeV)
0
2
4
6
8
10
12
0
5
10
15
20

Fig. 4

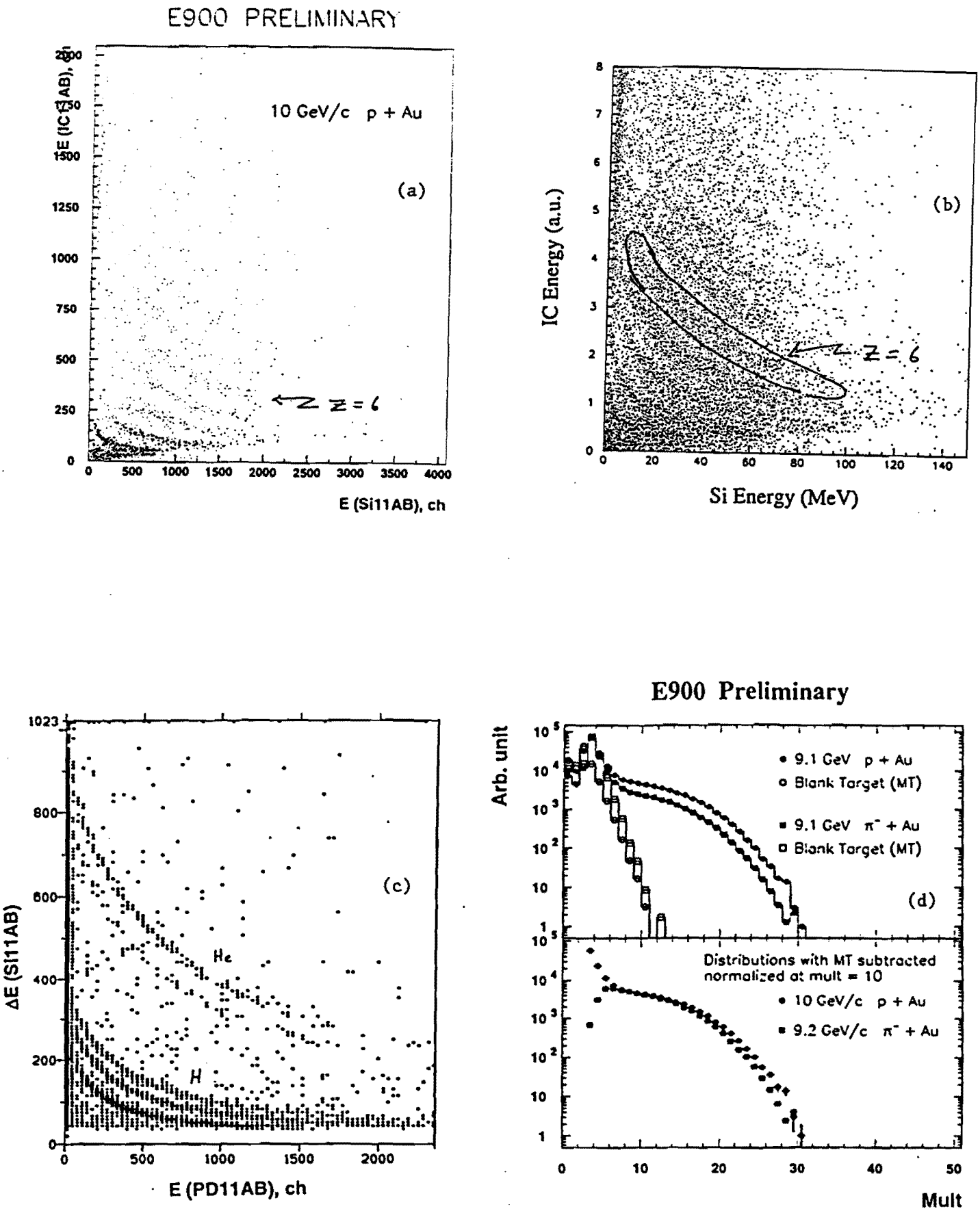
E900 PRELIMINARY
10 GeV/c p + Au
(a)
Z = 6
E (Si11AB), ch
(b)
IC Energy (a.u.)
Si Energy (MeV)
Z = 6
(c)
He
H
ΔE (Si11AB)
E (PD11AB), ch
E900 Preliminary
Arb. unit
9.1 GeV p + Au
Blank Target (MT)
9.1 GeV π⁻ + Au
Blank Target (MT)
(d)
Distributions with MT subtracted normalized at mult = 10
10 GeV/c p + Au
9.2 GeV/c π⁻ + Au
Mult

Fig.5

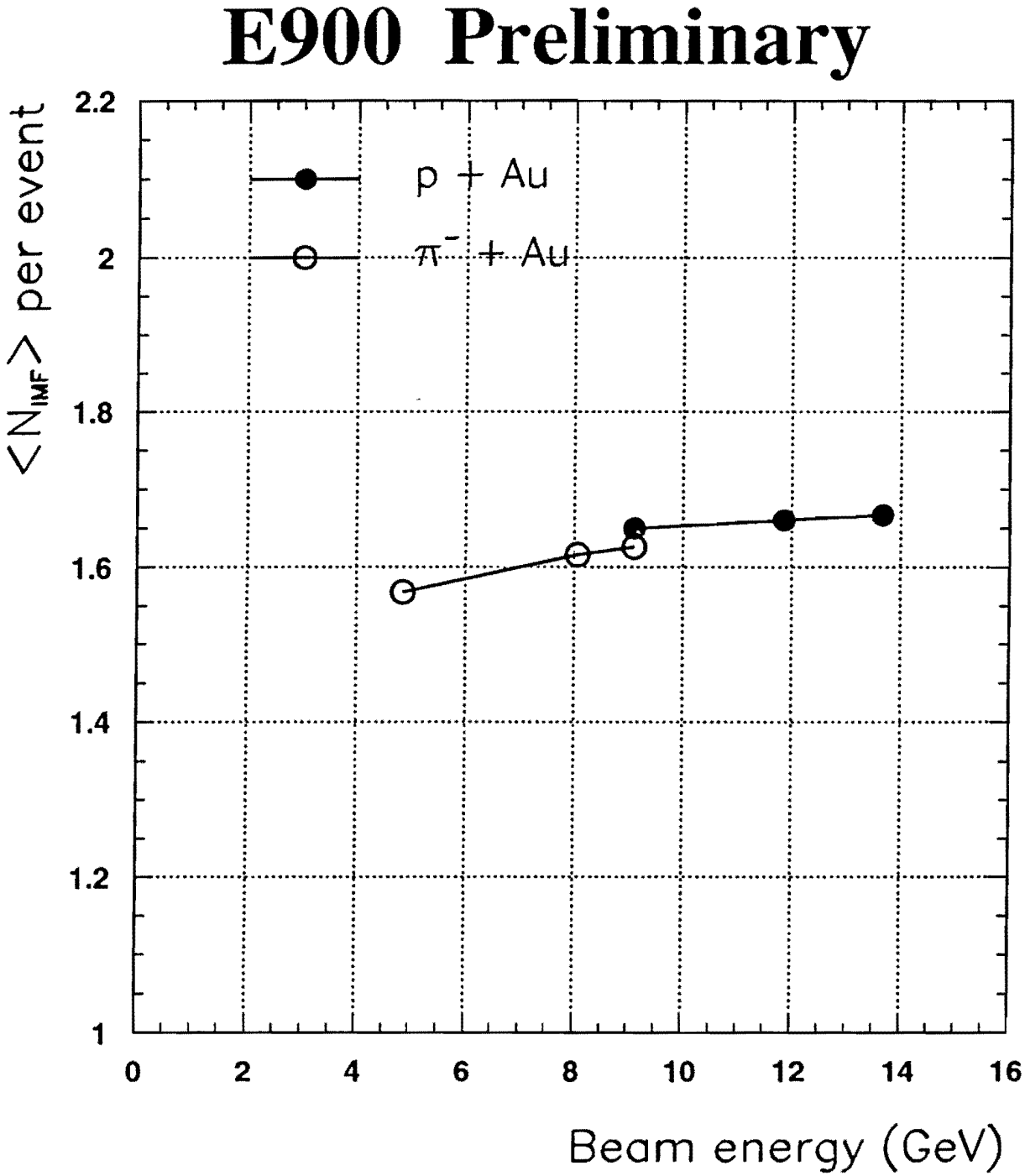
E900 Preliminary
p + Au
π⁻ + Au
<N_IMF> per event
Beam energy (GeV)
2.2
2
1.8
1.6
1.4
1.2
1
0
2
4
6
8
10
12
14
16

Fig. 6

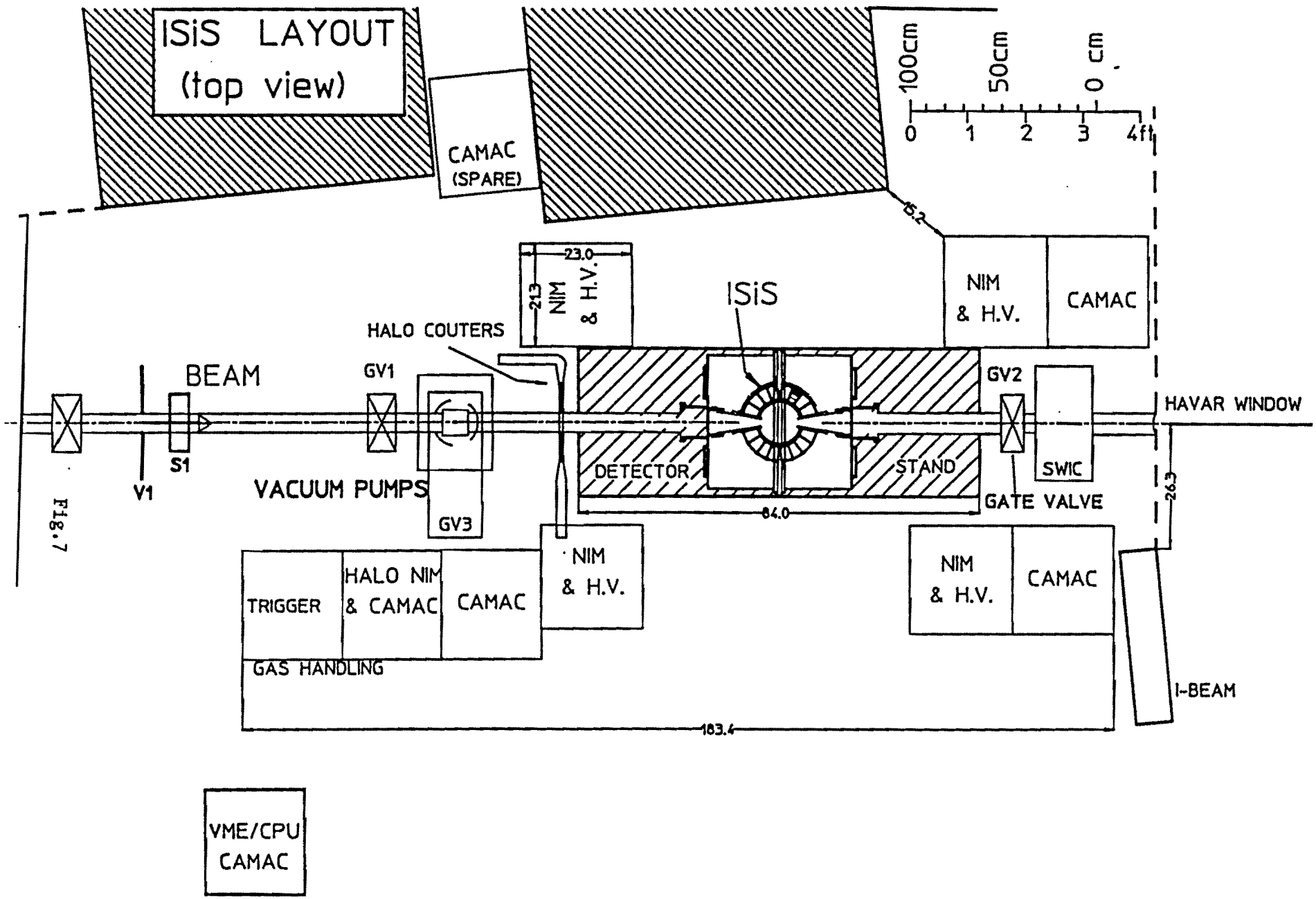
ISiS LAYOUT
(top view)
CAMAC
(SPARE)
100cm
50cm
0 cm
0
1
2
3
4ft
15.2
23.0
21.3
NIM
& H.V.
ISiS
NIM
& H.V.
CAMAC
HALO COUTERS
BEAM
GV1
GV2
HAVAR WINDOW
S1
V1
VACUUM PUMPS
GV3
DETECTOR
STAND
SWIC
GATE VALVE
84.0
26.3
NIM
& H.V.
TRIGGER
HALO NIM
& CAMAC
CAMAC
GAS HANDLING
NIM
& H.V.
CAMAC
I-BEAM
183.4
VME/CPU
CAMAC

Fig.7